Catalytic Mechanism of Dihydrofolate Reductase Enzyme. A Combined Quantum-Mechanical/Molecular-Mechanical Characterization of Transition State Structure for the Hydride Transfer Step

R. Castillo, J. Andrés, and V. Moliner*

Contribution from the Departament de Ciències Experimentals, Universitat Jaume I, Castelló, Spain

Received December 14, 1998. Revised Manuscript Received October 6, 1999

Abstract: A transition structure for the hydride transfer step in dihydrofolate reductase has been characterized in hybrid quantum-mechanical/molecular-mechanical (QM/MM) calculations involving a fully flexible active-site region by means of the GRACE software. The results are compared with in vacuo calculations and the importance of including the environment effect is stressed. Thus, while a degeneracy endo and exo transition structure is obtained in the gas phase calculations, the protein environment selectively moulds the substrate in a conformation close to the exo transition structure. The enzyme compresses the substrate and the cofactor into a conformation close to the transition structure, thus facilitating the hydride transfer. The population analysis obtained by means of the in vacuo and the hybrid QM/MM methods renders similar net atomic charges for the donor and acceptor fragments, suggesting that a hydrogen more than a hydride ion is transferred. When the environment effect is included it allows the role of the Asp27 in stabilizing the cationic pteridine ring to be demonstrated, while the ordered structure of the X-ray crystallographic water molecules supports the hypothesis of an indirect transfer of a proton from Asp27 residue to the N5 atom of the substrate. A good agreement between experimental and QM/MM primary kinetic isotope effects is found. The comparison of the results obtained with the different methods and models shows that while some common features are observed, for reactions involving a large number of degrees of freedom it is not correct to refer to one unique transition structure. The transition state should be considered as an average of nearly degenerated transition structures.

Introduction

Dihydrofolate reductase (5,6,7,8-tetrahydrofolate: NADP oxidoreductase, E.C. 1.5.1.3) catalyzes the NADPH-dependent reduction of 7,8-dihydrofolate (DHF) to 5,6,7,8-tetrahydrofolate (THF) in both bacterial and vertebrate cells. This enzyme is necessary for maintaining intracellular pools of THF and its derivatives, which are essential cofactors in the biosynthesis of several amino acids. This property has made DHFR a clinical target for antitumor and antiinfective therapy, and numerous inhibitors have been described.[1,2] Nevertheless, the details of the enzyme molecular reaction mechanism are still unclear and can only be hypothesized at present.[3,4]

The mechanism of the reaction requires the addition of both a proton and a hydride ion. Asp 27, in *Escherichia coli* dihydrofolate reductase (ecDHFR), is considered as the only group in the active site capable of providing the proton for the reduction of the N5−C6 bond,[5] although it is not clear enough if it takes place directly or through a series of water molecules.[6] In fact, mutation of this residue to a less acidic one (asparagine or serine) results in greatly diminished activity toward dihydrofolate at pH 7, but comparable activity to native DHFR at pH values sufficiently low to protonate dihydrofolate in solution.[5] The presence of a solvent channel with a series of ordered water molecules hydrogen bonded to the substrate and the protein and the fact that Asp 27 was too far from the N5 (the proton acceptor atom) support the hypothesis of an indirect protonation occurring. Nevertheless, as various mechanisms for this proton shuttling between Asp27 and N5 have been proposed,[7−11] and as a substrate binding role has also been conferred to the Asp 27 residue,[12] further studies are merited to clarify this hypothesis. It is generally accepted that the protonation precedes hydride ion transfer and activates the substrate,[13−16] thus being a strongly pH dependent chemical reaction.[6] The hydride comes from C4 of the dydronicotinamide ring of NADPH and the C6 of a protonated DHF (see Figure 1).

The exact characterization of stationary points such as minima, associated with reactants, products, and possible

(1) Blakley, R. L. *Folates and Pterins*; Wiley: New York, 1984.
(2) Fierke, C. A.; Johnson, K. A.; Benkovic, S. J. *Biochemistry* **1987**, *26*, 4085.
(3) Kraut, J.; Matthews, D. A. In *Biological Macromolecules and Assemblies*; Jurnak, F. A., McPherson, A., Eds.; Wiley: New York, 1987.
(4) Cummins, P. L.; Ramnarayan, K.; Singh, U. C.; Gready, J. E. *J. Am. Chem. Soc.* **1991**, *113*, 8247.
(5) Howell, E. E.; Villafranca, J. E.; Warren, M. S.; Oatley, S. J.; Kraut, J. *Science* **1986**, *231*, 1123.
(6) Cannon, W. R.; Garrison, B. J.; Benkovic, J. *J. Am. Chem. Soc.* **1997**, *119*, 2386.
(7) Howell, E. E.; Warren, M. S.; Booth, C. L. J.; Villafranca, J. E.; Kraut, J. *Biochemistry* **1987**, *26*, 8591.
(8) Morrison, J. F.; Stone, S. R. *Biochemistry* **1988**, *27*, 5499.
(9) Uchimaru, T.; Tsuzuki, S.; Tanabe, K.; Benkovic, J.; Furukawa, K.; Taita, K. *Biochem. Biophys. Res. Commun.* **1989**, *161*, 64.
(10) Bystroff, C.; Oatley, S. J.; Kraut, J. *Biochemistry* **1990**, *29*, 3263.
(11) McTigue, M. A.; Davies, I., J. F.; Kaufman, B. T.; Kraut, J. *Biochemistry* **1992**, *31*, 7264.
(12) Chen, Y.; Kraut, J.; Callender, R. *Biophys. J.* **1997**, *72*, 936.
(13) Gready, J. E. *Biochemistry* **1985**, *24*, 4761.
(14) Gready, J. E.; Cummins, P. L.; Wormell, P. *Adv. Exptl. Med. Biol.* **1993**, *338*, 487.
(15) Ivery, M. T. G.; Gready, J. E. *Biochemistry* **1995**, *34*, 3724.
(16) Jeong, S. S.; Gready, J. E. *Biochemistry* **1995**, *34*, 3734.

10.1021/ja9843019 CCC: $18.00
Published on Web 12/14/1999

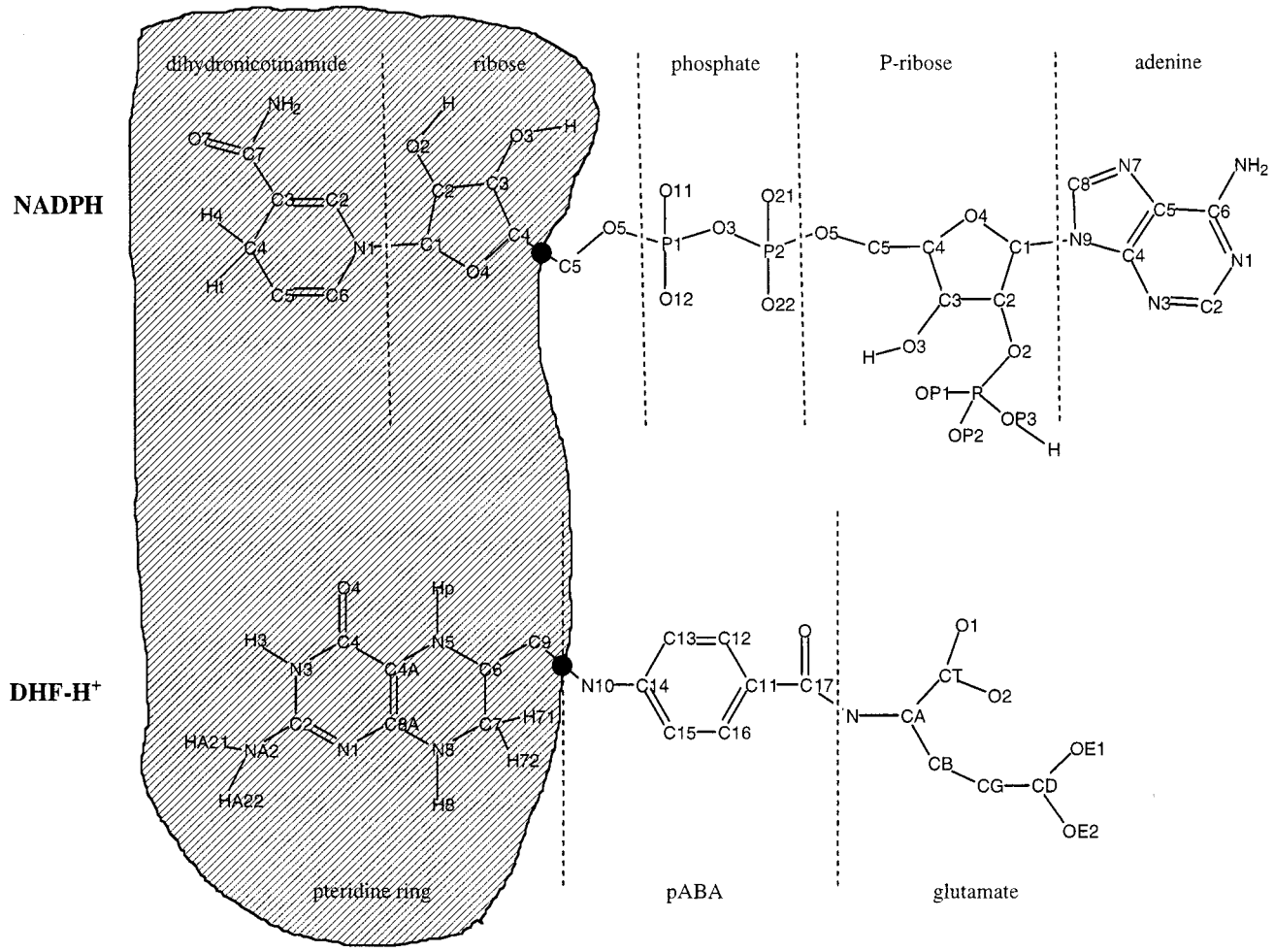

Figure 1. Covalent structure and standard atomic numbering for cofactor (NADPH) and substrate (protonated DHF: $DHF-H^+$). Hydrogen quantum link atoms, indicated as "●", divide the quamtum (shaded area) and classical regions.

intermediates, and transition structure (TS) on potential energy surface by means of calculations of analytical gradients and second derivatives of the energy with respect to geometric parameters is a powerful tool to help check for different molecular mechanisms related to enzyme phenomena. In a previous study on horse liver alcohol dehydrogenase,[18,19] we found that neither the relaxed products nor the reactants of the substrate system could be docked at the corresponding active site; but the TS, calculated in a vacuum, just fitted there. Since then, not only complementarity in shape to active sites as proposed by Pauling in the forties[20] but also invariances of TS to molecular model size, level of electronic theory, and surrounding medium effects have been identified for several reaction mechanisms.[17,21−31] In this study we report the results of a combined classical/quantum modeling study for reduction of 5,6-dihydrofolate catalyzed by ecDHFR, being the key point in the characterization of the TS associated with the hydride transfer step.

Factors influencing hydride transfer geometry have been well discussed by Williams et al.[32] In this sense, the endo structure seems to be a general feature on hydride transfer steps understood in terms of the frontier orbital overlap of the donor and acceptor centers in the saddle point.[17,33−38] These results are in agreement with our previous in vacuo MO calculations for the hydride transfer step in the DHFR-like reaction.[39−41] Nevertheless, as the result of a large conformational search in

(17) Tapia, O.; Cárdenas, R.; Andrés, J.; Colonna-Cesari, F. *J. Am. Chem. Soc.* **1988**, *110*, 4046.
(18) Plapp, B. V.; Eklund, H.; Brändén, C. I. *J. Mol. Biol.* **1978**, *122*, 23.
(19) Eklund, H.; Plapp, B. V.; Samama, J. P.; Brändén, C. I. *J. Bio. Chem.* **1982**, *257*, 14349.
(20) Pauling, L. *Nature* **1948**, *161*, 707.
(21) Tapia, O.; Jacob, O.; Colonna-Cesari, F. *Theor. Chim. Acta* **1992**, *82*, 217.
(22) Tapia, O.; Andrés, J.; Cárdenas, R. *Chem. Phys. Lett.* **1992**, *189*, 395.
(23) Tapia, O.; Andres, J. *Mol. Eng.* **1992**, *2*, 37.
(24) Jacob, O.; Tapia, O. *Int. J. Quantum Chem.* **1992**, *42*, 1271.
(25) Tapia, O.; Jacob, O.; Colonna, F. *Theor. Chim. Acta* **1993**, *85*, 217.
(26) Andrés, J.; Moliner, V.; Krechl, J.; Silla, E. *J. Phys. Chem.* **1994**, *98*, 3664.
(27) Tapia, O.; Andrés, J.; Safont, V. S. *J. Phys. Chem.* **1994**, *98*, 4821.
(28) Andrés, J.; Moliner, V.; Safont, V. S. *J. Chem. Soc., Faraday Trans.* **1994**, *90*, 1703.
(29) Tapia, O.; Andres, J.; Safont, V. S. *J. Phys. Chem.* **1996**, *100*, 8543.
(30) Safont, V. S.; Oliva, M.; Andres, J.; Tapia, O. *Chem. Phys. Lett.* **1997**, *278*, 291.
(31) Moliner, V.; Andrés, J.; Oliva, M.; Safont, V. S.; Tapia, O. *Theor. Chem. Acc.* **1998**, in press.
(32) Williams, I. H.; Miller, A. B.; Maggiora, G. M. *J. Am. Chem. Soc.* **1990**, *112*, 530.
(33) Wu, Y.-D.; Houk, K. N. *J. Am. Chem. Soc.* **1987**, *109*, 2226.
(34) Wu, Y.-D.; Houk, K. N. *J. Am. Chem. Soc.* **1987**, *109*, 906.
(35) Wu, Y. D.; Houk, K. N. *J. Am. Chem. Soc.* **1991**, *113*, 2353.
(36) Almarsson, Ö.; Karaman, R.; Bruice, T. C. *J. Am. Chem. Soc.* **1992**, *114*, 8702.
(37) Almarsson, Ö.; Bruice, T. B. *J. Am. Chem. Soc.* **1993**, *115*, 2125.
(38) Houk, K. N.; González, J.; Li, Y. *Acc. Chem. Res.* **1995**, *28*, 81.
(39) Andrés, V.; Safont, V. S.; Martins, J. B. L.; Beltrán, A.; Moliner, V. *J. Mol. Struct. THEOCHEM* **1995**, *330*, 411.
(40) Andrés, V.; Moliner, V.; Safont, V. S.; Domingo, L. R.; Picher, M. T.; Krechl, J. *Bioor. Chem.* **1996**, *24*, 10.

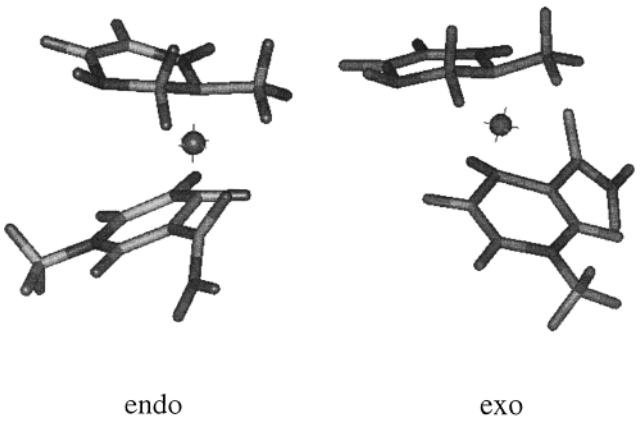

Figure 2. Transition state structures for the hydride transfer step in a model of the DHFR catalyzed reaction, obtained with the in vacuo AM1 semiempirical method.

the quadratic region of the in vacuo potential energy surface (PES), we have located and characterized a TS with an exo configuration (see Figure 2). To understand which structure is "preferred" by the enzyme and the role of the protein environment we have employed a hybrid theoretical technique in which a quantum-mechanical (QM) description of the chemical bond making and breaking events is combined with a molecular mechanical (MM) treatment of the surrounding protein and solvent. A new computational procedure is employed, which allows the TS to be located with full gradient relaxation of the positions of ca. 3000 atoms of a solvated enzyme−substrate complex utilizing a Hessian involving displacements of 53 atoms in the active site. The resulting TS shows remarkable structural similarity to that determined in earlier calculations for the reaction studied in vacuo.[39−41]

Computational Details

In vacuo calculations were carried out with the GAUSSIAN94 package of programs,[42] performed at the Hartree−Fock (HF) level of theory using the standard 4-31G basis set, and by means of the AM1 semiempirical Hamiltonian. The exact location of the TS was achieved by using an algorithm, in which the coordinates describing the system are separated into two sets: the control space, which is responsible for the unique negative eigenvalue in the respective force constants matrix, and the remaining coordinates set that is called complementary space. The geometry optimizations are carried out alternatively on each subspace, one at a time, until a stationary structure is obtained. Finally, a complete analytical optimization of the TS was achieved for the complete space of all variables. At this point, the "eigenvector following" optimization method was used. The nature of each stationary point was checked by diagonalizing the Hessian matrix to determine the number of imaginary frequencies (zero for the local minima and one for the TSs). The in vacuo molecular model was built with an *N*-methylated nicotinamide ring, representing the NADPH cofactor, and a protonated pteridine ring that mimics the substrate.

The QM/MM energy hypersurface was obtained using the CHARMM24 program[43] as described previously for reactions in aqueous solution[44] and in solvated enzyme active sites.[31,45,46] The starting geometry comes from the 1.6 Å resolution ternary complex X-ray crystal structure of an *Escherichia coli* DHFR (ecDHFR−NADPH−Folate).[47] CHARMM24 was also used to add hydrogens to all titratable residues at a state complementary to pH 7. The system was placed in a cavity deleted from a preformed 18 Å radius sphere of TIP3P[48] water molecules centered on the donor and acceptor carbon atoms. Once the entire system was built, and due to computational limitations, two different truncations were performed: (I) to delete part of the system (those atoms 18 Å away from the active site) and then to apply a harmonic force to those heavy atoms in the surroundings of the resulting pseudo-sphere molecular model and (II) to keep the full number of enzyme heavy atoms of the initial structure, but freezing the position of the atoms deleted in model I. The first procedure provides a more flexible model, while the second one would allow us to mimic very long distance interactions. The resulting model I was a pseudosphere of 3139 atoms of enzyme, cofactor, substrate, and solvent centered around the hydride donor and acceptor atoms. Harmonic restraints were applied to a total of 415 atoms to maintain the structure of the enzyme where the truncation produced odd ends. Model II consists of 3385 atoms, 661 of them kept frozen. Both models were divided into a QM region, treated by the AM1 semiempirical MO method, and a MM region comprising the rest of the protein (CHARMM24 potentials) and the water molecules. Two hydrogen "link atoms",[49] where covalent bonds cross the boundary between the QM and the MM regions, were added to satisfy the valence of the QM fragments. The structural formula of N5 protonated DHF (DHF−H^+) and the cofactor NADPH are depicted in Figure 1, where the quantum link atoms are indicated as "●". The QM region, formed by the dihydronicotinamide ring, the ribose ring, and the substituted pteridine ring (shown as the shaded portion of Figure 1), contained a total of 53 atoms. Finally, a QM/MM energy minimization was performed to obtained a reactant-like structure.

A grid scanning (defined by two internal coordinates: the donor−acceptor atoms distance and the Ht−acceptor atoms distance) was used for the initial phase of the saddle-point search procedure. Once the potential energy surface was obtained, a localized approximate TS was refined using the recently developed GRACE software.[46,50] A partial-rational-function-operator/adopted-basis-Newton−Raphson method was employed, utilizing a Hessian matrix of order 159 × 159, describing the curvature of the QM/MM energy hypersurface for a subset of the system, together with a diagonal Hessian plus updates for the rest of the system. The root-mean-square residual gradient on the 53 atoms in the subset is less than 0.1 kcal/mol $Å^{-1}$ in the optimized structure, while on the remaining atoms (ca. 3000) it is less than 0.005 kcal/mol $Å^{-1}$; these residual gradients are lower than the commonly accepted convergence criterion for optimized geometries of small molecules in quantum chemistry.[51] Finally, the intrinsic reaction coordinate (IRC)[52] path was traced from the TS in each direction, leading to DHF−H^+ and to THF, to demonstrate conclusively that the reported structure is indeed a TS for the correct reaction.

Results and Discussion

The in vacuo optimized endo and exo TSs are shown in Figure 2, while a detail of the refined QM/MM TS is depicted in Figure 3. Table 1 reports some relevant parameters of the optimized TSs, concerning the chemical reaction itself, obtained

(41) Andrés, V.; Moliner, V.; Safont, V. S.; Aulló, J. M.; Diaz, W.; Tapia, O. *J. Mol. Struct. THEOCHEM* **1996**, *371*, 299.
(42) Frisch, M. J.; Trucks, G. W.; Schlegel, H. B.; Gill, P. M. W.; Johnson, B. G.; Robb, M. A.; Cheeseman, J. R.; Keith, T.; Peterson, G. A.; Montgomery, J. A.; Raghavachari, K.; Al-Laham, M. A.; Zakrzewski, V. G.; Ortiz, J. V.; Foresman, J. B.; Cioslowski, J.; Stefanov, B. B.; Nanayakkara, A.; Challacombe, M.; Peng, C. Y.; Ayala, P. Y.; Chen, W.; Wong, M. W.; Andres, J. L.; Replogle, E. S.; Gomperts, R.; Martin, R. L.; Fox, D. J.; Binkley, J. S.; Defrees, D. J.; Baker, J.; Stewart, J. P.; Head-Gordon, M.; Gonzalez, C.; Pople, J. A. In Gaussian Inc.: Pittsburgh, PA, 1995.
(43) Brooks, B. R.; Bruccoleri, R. E.; Olafson, B. D.; States, D. J.; Swaminathan, S.; Karplus, M. *J. Comput. Chem.* **1983**, *4*, 187.
(44) Barnes, J. A.; Williams, I. H. *J. Chem. Soc., Chem. Commun.* **1996**, 193.
(45) Barnes, J. A.; Williams, I. H. *Biochem. Soc. Trans.* **1996**, *24*, 263.
(46) Moliner, V.; Turner, A. J.; Williams, I. H. *J. Chem. Soc., Chem. Commun.* **1997**, 1271.
(47) Sawaya, M. R.; Kraut, J. *Biochemistry* **1997**, *36*, 586.
(48) Jorgensen, W. L.; Chandrasekhar, J.; Madura, J.; Impey, R. W.; Klein, M. L. *J. Chem. Phys.* **1983**, *79*, 926.
(49) Field, M. J.; Bash, P. A.; Karplus, M. *J. Comput. Chem.* **1990**, *11*, 700.
(50) Turner, A. J. Doctoral Thesis, University of Bath, 1997.
(51) Foresman, J. B.; Frisch, A. E. *Exploring Chemistry with Electronic Structure Methods*; Gaussian, Inc.: Pittsburgh, PA, 1993.
(52) Fukui, K. *J. Phys. Chem.* **1970**, *74*, 4161.

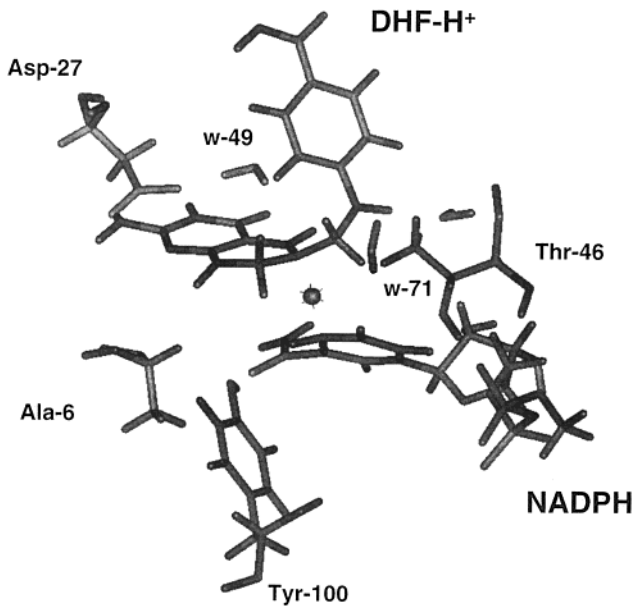

Figure 3. Detail of the QM/MM TS refined using GRACE for the hydride transfer step of the DHFR catalyzed reaction.

with the different methods and models. According to these result, the active site of the enzyme moulds the substrate and the cofactor in an exo-like conformation, slightly different from the exo TS obtained in vacuo (see the dihedral angle defined by the C8A−C6−C4−N1 atoms), and not into an endo conformation that was energetically favored in vacuo. Due to steric impediments, the conformational degeneracy of the TS observed in vacuo is not render by the QM/MM calculations, where H-bonds and mechanical interactions between the substrate and the amino acids of the active site limit the conformations.

A comparison between simple and sophisticated models and methods shows, nevertheless, some remarkably similarities. There is a minimal molecular model associated with geometrical parameters describing the essentials of the chemical interconversion step, i.e., the corresponding geometrical parameters of TS and the components of the unique imaginary frequency associated with the transition vector. This set of parameters coincides with what we have called "control space" in the previous section. In this sense, the distances between donor and acceptor carbon atoms, C6−C4, obtained with all models and methods are in a range of 0.111 Å: the 2.632 Å value of the endo TS obtained by means of the HF method would be the lower limit while the 2.751 Å value of the QM/MM calculations using model II corresponds to the higher value. The position of the hydride ion, defined by the C4−Ht distance and the donor−hydride−acceptor bond angle (C6−Ht−C4), also looks to be a common feature ranging between 1.405 and 1.345 Å and between 156.8 and 168.7°, respectively. This later angle was found to be in the range 140−168° for different hydride transfer steps in enzyme reaction mechanisms studied previously by us and other workers (see ref 41 and papers cited therein). All values reported in Table 1 fit into this interval.

In Table 2 lists some interatomic distances in the reactant, TS, and product obtained from the QM/MM calculations using model I and model II. An analysis of the results suggests that both substrate and cofactor are H-bonded to the protein backbone in the three states by means of different residues. Distances between residues such as the Asp27 and the substrate reveal a strong interaction (OD1 and OD2 of Asp27 with HA21 and H3 of the pteridine ring, respectively). Most of the distances between the protein and the substrate remain constants on going from reactants to TS and products. These results support the hypothesis of an active site pocket that compresses the substrate into a conformation structure closer to the TS than to the in vacuo reactants-like structure. The crystal water molecules also seem to be in ordered positions, capable of working as the solvent channel suggested by Cannon and co-workers for the previous proton step.[6] In this regard, as presented in Table 2, water 49 (w-49) is in the standard H-bond distances from O4 and Asp27 (not presented in the table). This water molecule, as well as w-71, could play a direct role in the network of waters that help to transfer the Hp from Asp27 to the N5−C6 bond, as suggested previously. Nevertheless, other parameters describing the relative position of the amino acids side chain (Arg 52 or Arg 98), the position of some water molecules (w-71, w-53, or w-42), or even the C8A−C6−C4−N1, which may be used as a guide of the endo or exo conformation, cannot be considered as "invariable"; the results obtained with model I are significantly different, in this regard, from those coming from model II. These discrepancies between one model and another are attributed to the nature of molecular systems with a large number of atoms thus giving many nearly degenerated structures: for enzyme reactions it is not worthwhile to talk about one unique TS. We rather refer to families of TS, all of them showing some invariances but with different conformations concerning the active-site residues. This result also has been observed in similar calculations carried out for the pyruvate reduction on the LDH active site.[53]

In addition to the mechanical effect of the active site, there is also a protein environment electrostatic contribution to the catalysis. The study of the net atomic charges, calculated with the help of Mulliken's population analysis using GAUSSIAN94 and CHARMM24 for the in vacuo and in enzyme models, respectively, allows similar conclusions to be obtained. They reveal a cationic character of the substrate in the ground state (see the "Sum=" values in Table 3, parts a and b) that diminishes from reactants to TS and products. This result confirms the well-known idea of a negative charge going from the dihydronicotinamide ring to the pteridine fragment, but as the Ht charge value suggests (close to zero), the nature of the hydride ion transferred seems to be, in fact, a hydrogen-like atom instead of a negative hydride ion. As explained in our previous work,[41] the transfer of an equivalent can be gathered into two different mechanisms: (i) a hydride ion mechanism and (ii) electron-transfer accompanied by a hydrogen atom migration. Our result, similar to those by Gready and co-workers[54,55] but in contrast to the analysis of hydride transfers in different model system carried out by Bertrán and co-workers in terms of valence bond structures,[56−58] provides evidence of a coupled hydrogen atom motion and charge transfer. A note of caution is necessary at this point: the standard quantum chemical methods used in this work to calculate the electronic structure are not adequate to determine the structure of a hydride ion.[59] Furthermore, as pointed out by Alhambra and co-

(53) Turner, A. J.; Moliner, V.; Williams, I. H. *J. Phys. Chem. Chem. Phys.* **1999**, *1*, 1323.
(54) Cummins, P. L.; Gready, J. E. *J. Comput. Chem.* **1990**, *11*, 791.
(55) Ranganathan, S.; Gready, J. E. *J. Chem. Soc., Faraday Trans.* **1994**, *90*, 2047.
(56) Mestres, J.; Lledos, A.; Durán, M.; Bertrán, J. *J. Mol. Struct. (THEOCHEM)* **1992**, *260*, 259.
(57) Mestres, J.; Durán, M.; Bertrán, J. *Theor. Chim. Acta* **1994**, *88*, 325.
(58) Mestres, J.; Durán, M.; Bertrán, J. *Bioorg. Chem.* **1996**, *24*, 69.
(59) Tapia, O.; Andres, J.; Aullo, J. M.; Bränden, C.-I. *J. Chem. Phys.* **1985**, *83*, 4673.

Table 1. Imaginary Frequencies, $\nu^{\ddagger}$ (cm^{-1}), Selected Interatomic Distances (Å), Angles (deg), and Dihedral Angles (deg) Obtained with the Different Methods and Models for the TS

	in vacuo					
	AM1		HF/4-31G		QM/MM	
	exo	endo	exo	endo	model I	model II
$\nu^{\ddagger}$	1205.7	1299.6	1491.4	1408.7	1378.0	1371.9
C6(pte.)−C4(nic.)	2.690	2.743	2.637	2.632	2.729	2.751
C4(nic.)−Ht	1.405	1.395	1.342	1.345	1.376	1.349
C6(pte.)−Ht−C4(nic.)	156.8	168.3	166.15	168.7	166.4	162.27
C8A−C6(pte.)−C4−N1(nic.)	220.0	351.3	218.18	351.3	229.6	135.34

Table 2. Interatomic Distances (Å) in Reactants, TS, and Products Obtained By Means of the QM/MM Calculations Using Model I and Model II

			model I			model II		
	QM atom	MM atom	R	TS	P	R	TS	P
substrate								
pteridine	NA2	Trp30 HC	2.81	2.89	3.10	2.85	2.83	2.63
	HA21	Asp27 OD1	1.72	1.82	1.83	1.76	1.79	1.77
	HA22	OW1	2.12	2.24	2.20	2.20	2.23	2.25
	N3	Ala7 HB2	2.82	2.74	2.96	3.09	2.98	3.22
	H3	Asp27 OD2	1.78	1.75	1.83	1.70	1.70	1.76
	O4	HW49	1.83	1.85	1.82	1.89	1.88	1.87
	Hp	OW71	2.08	2.12	3.07	5.55	5.20	5.35
	H71	Ile94 O	2.47	2.38	2.01	2.39	2.29	2.32
	H8	Ile5 O	1.84	1.90	2.01	1.80	1.80	1.87
pABA	H10	OW128	1.71	1.74	1.78	1.90	1.86	1.74
glutamate	O1	Arg57 HH11	1.67	1.68	1.68	1.68	1.68	1.68
	O2	Lys32 HZ1	1.80	1.79	1.78	1.73	1.74	1.74
	O2	Arg52 HH12	1.69	1.68	1.68	4.18	4.17	4.16
	O2	Arg57 HH22	1.79	1.78	1.79	1.79	1.80	1.81
	O2	HW108	1.65	1.65	1.65	1.73	1.73	1.72
	OE2	Lys32 HZ3	1.61	1.62	1.62	1.65	1.66	1.65
	OE1	HW102	1.69	1.69	1.69	1.64	1.64	1.64
	OE2	HW138	1.65	1.64	1.64	1.62	1.62	1.62
NADPH								
dihydronic	O7	Ala6 HA	2.48	2.59	2.66	2.40	2.47	2.24
	O7	Tyr100 HN	2.02	2.06	2.05	2.04	2.09	2.01
ribose	H4	OW53	2.59	2.58	2.56	2.41	2.41	2.38
	HO3	OW53	2.80	2.80	2.90	1.90	1.89	1.94
	O2	HW44	2.60	2.62	2.63	3.26	3.45	3.41
phosphate	O21	Thr46 HN	2.09	2.20	2.17	2.02	2.06	2.06
	O21	Thr46 HG1	1.61	1.61	1.57	1.59	1.59	1.55
	O3	His45 HD2	2.48	2.49	2.66	2.55	2.57	2.57
	O3	His45 HB2	2.34	2.33	2.33	2.30	2.31	2.31
	O12	HW5	1.64	1.65	1.66	1.71	1.69	1.75
P-ribose	O4	Arg44 HN	1.80	1.79	1.80	1.86	1.86	1.88
	O3	Arg98 HH11	1.99	2.00	2.01	3.22	3.42	3.42
	OP1	Arg44 HH21	1.75	1.74	1.74	1.78	1.78	1.78
	OP2	HW52	1.64	1.81	1.81	1.77	1.77	1.77
adenine	N1	HW42	1.94	1.94	1.94	5.34	4.45	4.47

workers,[60] in the original implementation of the link-atom approach,[49] electrostatic interactions between the link atom and the rest of the protein atoms were not included in the quantum calculation. This, however, introduces an imbalance in electrostatic interactions in the QM region due to the fact that molecular orbitals are delocalized, and such a partition, which excludes some terms in the Fock matrix, results in unrealistically large partial charges on link atoms and the atoms they are attached to. This deficiency, inherit in CHARMM link-atom treatment, always has to be kept in mind and conclusions must be discused with caution unless a correction is taken into account (see ref 60).

In this work, it is nevertheless true that the quantum link atom charges are constant in the three states (ca. −0.9 au), so no change in the polarization has been induced by the MM charges from reactants to TS and products. This result means that a minimal artifact result is obtained by the presence of these virtual H atoms in relative magnitudes.

From the results listed in Table 3 it is also possible to understand the putative function of the Asp 27 stabilizing the protonated substrate, as revealed by Raman difference spectroscopy studies of Callender et al.[12] If we focus our interest on the C6−N5 bond, the polarization of the C6−N5 bond toward the TS is demonstrated, thus facilitating the hydride transfer.

The inclusion of the environment effect by means of this flexible QM/MM model can render more information. The IRC path traced from the TS in the DHF−H^+ direction leads to a reactant-like structure. This minimum, when using the in vacuo calculations, corresponds to a reactant complex with a C6−C4 distance significantly longer (see Table 4). Crystal structures of dead-end *E. Coli* DHFR·$NADP^+$·folate obtained by Kraut

(60) Alhambra, C.; Wu, L.; Zhang, Z.; Gao, J. *J. Am. Chem. Soc.* **1998**, *120*, 3858.

Table 3. Net Atomic Charges on the Substrate and Cofactor Moieties

	pteridine ring				dihydronicotinamide ring		
	R	TS	P		R	TS	P
(a) QM/MM Calculations Using Model I							
N1	−0.34	−0.31	−0.30	N1	−0.20	−0.13	−0.05
C2	0.29	0.24	0.20	C2	0.10	0.07	0.03
NA2	−0.35	−0.35	−0.35	H2	0.16	0.18	0.21
HA21	0.30	0.28	0.27	C3	−0.35	−0.29	−0.17
HA22	0.26	0.23	0.22	C7	0.38	0.39	0.37
N3	−0.34	−0.34	−0.33	O7	−0.54	−0.52	−0.49
H3	0.34	0.33	0.31	N7	−0.42	−0.40	−0.37
C4	0.40	0.37	0.36	H71	0.23	0.25	0.28
O4	−0.42	−0.44	−0.45	H72	0.23	0.25	0.23
C4A	−0.37	−0.21	−0.18	C4	−0.03	0.07	−0.03
N5	0.08	−0.16	−0.21	H4	0.04	0.13	0.18
Hp	0.39	0.35	0.28	Ht	0.06	0.00	0.06
C6	0.02	0.06	−0.06	C5	−0.33	−0.30	−0.18
C7	−0.05	−0.07	−0.08	H5	0.16	0.19	0.22
H71	0.09	0.08	0.07	C6	0.04	0.09	0.11
H72	0.17	0.11	0.09	H6	0.29	0.32	0.35
N8	−0.31	−0.31	−0.30	ribose	1.11	1.16	1.22
H8	0.31	0.27	0.24	link_H	−0.91	−0.92	−0.92
C8A	0.27	0.15	0.07	sum =	0.02	0.54	1.05
C9	0.93	0.92	0.90				
H91	0.14	0.10	0.06				
H92	0.09	0.06	0.04				
link_H	−0.90	−0.89	−0.89				
sum =	0.94	0.46	−0.06				
(b) In Vacuo AM1 Calculations[a]							
C4A	−0.33	−0.19	−0.13	N1	−0.34	−0.28	−0.19
H4	0.29	0.26	0.22	CH_3	0.25	0.30	0.34
N5	−0.17	−0.37	−0.39	C2	0.05	0.03	−0.03
Hp	0.41	0.36	0.28	H2	0.21	0.26	0.29
C6	0.07	0.11	−0.04	C3	−0.31	−0.28	−0.17
CH_3	0.23	0.13	0.06	$CONH_2$	−0.07	0.05	0.12
C7	−0.10	−0.15	−0.17	C4	−0.12	0.01	−0.03
H71	0.19	0.17	0.14	H4	0.14	0.23	0.32
H72	0.19	0.15	0.14	Ht	0.12	0.03	0.09
N8	−0.46	−0.40	−0.38	C5	−0.28	−0.30	−0.20
H8	0.35	0.28	0.23	H5	0.21	0.26	0.30
C8A	0.05	−0.13	−0.27	C6	−0.07	−0.03	−0.05
H8A	0.27	0.25	0.21	H6	0.23	0.26	0.29
sum =	0.99	0.47	−0.10	sum =	0.02	0.54	1.08

[a] The reactants, TS, and products correspond to the exo-like structures.

and co-workers[61] reveal a distance of 3.1 Å, what could be considered as a ground-state structure. This value is shorter than that in the reactants structure but longer than the distance in the TS. As pointed out by the authors, the pteridine and nicotinamide rings must, therefore, move still closer together from their ground-state positions to the TS. In any case, the QM/MM results appear to be closer to the crystal structures than those of the in gas-phase calculations, what make the hybrid QM/MM model a more realistic theoretical approach. It could be said that the enzyme keeps the substrate in the vicinity of the quadratic region of the saddle point. The approach of the two donor and acceptor atoms is helped by the relative twisting between the pteridine and nicotinamide rings (the C8A−C6−C4−N1 dihedral angle remains almost constant). Other geometrical changes occur as the carboxamide group of the nicotinamide (defined by the C4−C3−C7−O7 dihedral angle) rotates ca. 30° from reactants to products, thus avoiding steric impediments and facilitating the approach of the donor acceptor atoms. Nevertheless, our TS results present a nicotinamide ring in an almost planar conformation, while Wu and Houk obtained a boat conformation using in vacuo theoretical studies of hydride-transfer reactions with a 1,4-dihydropyridine ring as a model for the hydride donor,[35] similar to the results of Almarson and co-workers.[36,37] We attribute this discrepancy to the fact that our QM/MM model is able to describe the steric effects, while in the gas-phase calculations, again, the donor moiety is not linked to the rest of the cofactor thus being free to move during the optimization.

These structural results are, obviously, associated with the energetics of the reaction. The in vacuo semiempirical and ab initio Hamiltonians predict an energy barrier between reactant complex and the exo transition state structure of 31 and 42 kcal/mol, respectively. The endo configuration appears to be energetically favored 2 and 8 kcal/mol in the AM1 and HF cases, respectively. These values are quite close to those obtained by Cummins and Gready in a very recent QM/MM free energy perturbation study of the hydride-ion transfer step in DHFR (ca. 30 kcal/mol).[62] Our QM/MM calculated energy barrier, 25.69 and 23.41 kcal/mol for models I and II, respectively, is slightly smaller than the in vacuo results. This trend is in accordance with the geometrical results; as we have pointed out, our QM/MM reactant-like structure is closer to the TS than the in vacuo reactants−TS gap. Nevertheless, a barrier energy of about 24 kcal/mol could be considered a high value for an enzyme reaction. At this point, we have to keep in mind that a semiempirical Hamiltonian is used for the QM region while, as Gao and co-workers suggest, it would be desirable to use ab initio molecular orbital or density functional theory in the hybrid QM/MM approach.[63] However, such computations are still too time-consuming to be practical for applications in molecular models involving such a number of degrees of freedom. Previous semiempirical vs ab initio comparative studies of in vacuo reaction demonstrated how the semiempirical Hamiltonians always rendered an energy barrier higher than the calculations where the correlation energy was taken into account, for instance, at the second-order Møller Pleset (MP2) level of theory.[26] Warshel and co-workers, in studies on quantum mechanical corrections for rate constants of hydride-transfer reactions in enzymes and solutions,[64,65] attribute the high activation free energy values to the non-inclusion of the quantum dynamical effects in this kind of calculation. In other terms, studies of the pH dependence of deuterium kinetic isotope effects (KIE) on the mechanism of this enzyme reaction carried out by Morrison and Stone revealed that the catalytic efficiency of ecDHFR was limited by product release at low and neutral pH and the catalysis slowed with increasing pH.[8] These results mean that the mayor contribution of the enzyme catalysis is not the hydride transfer step, so we cannot expect a dramatic decrease in its energy barrier.

To check in some way our optimized structures, we have computed QM/MM primary deuterium KIEs for substitution of the transferring hydrogen NADPH/NADPD by using the partition functional of reactants and TS and assuming the transition state theory.[66] Thus, semiclassical KIE are obtained from the partition functions of reactants and the transition state for the 53 atoms in the "control" subset in the presence of the force field made by the rest of the MM atoms. The rigid-rotor/

(61) McTigue, M. A.; Davies, I. J. F.; Kaufman, B. T.; Kraut, J. *Biochemistry* **1993**, *32*, 6855.

(62) Cummins, P. L.; Gready, J. E. *J. Comput. Chem.* **1998**, *19*, 977.

(63) Gao, J.; Freindorf, M. *J. Phys. A* **1997**, *101*, 3182.

(64) Kong, Y. S.; Warshel, A. *J. Am. Chem. Soc.* **1995**, *117*, 6234.

(65) Hwang, J. K.; Chu, Z. T.; Yadav, A.; Warshel, A. *J. Phys. Chem.* **1991**, *95*, 8445.

(66) Glasstone, K. J.; Laidler, K. J.; Eyring, H. *The Theory of Rate Processes*; McGraw-Hill: New York, 1941.

Table 4. Selected Interatomic Distances (Å), Angles (deg), and Dihedral Angles (deg) Obtained with the Different Methods and Models for the Reactants Structure

	in vacuo					
	AM1		HF/4-31G		QM/MM	
	exo	endo	exo	endo	model I	model II
C6(pte.)−C4(nic.)	5.043	4.379	5.029	4.974	3.293	3.876
C4(nic.)−Ht	1.127	1.127	1.087	1.087	1.116	1.119
C6(pte.)−Ht−C4(nic.)	139.77	128.63	125.55	108.82	150.07	106.59
C8A−C6(pte)−C4−N1(nic)	124.74	117.22	151.66	62.96	129.15	134.67

harmonic-oscillator approximations were used with the CAMVIB/CAMISO programs[67,68] to calculate the effects of replacing the transferring hydrogen atom by a deuterium. The results (k_1/k_2) at 298 K are 3.735 and 3.896 for models I and II, respectively. These theoretical values are comparable to the experimental work of Morrison and Stone, who observed a limiting deuterium KIE value of about 3.0 at pH 10.2, which made them conclude that the hydride transfer became, at least, partly rate-limiting.[8] Unfortunately, this means that a direct comparison between experimental and predicted KIE must be taken with caution as the hydride transfer step in DHFR is not the rate-limiting step at pH 7 (the pH we selected to add hydrogens to all ionizable groups of the amino acids), or at pH 10. Nevertheless, previous KIE calculations carried out by us for several in vacuo models of the hydride transfer step related to enzyme processes (LADH,[69] LDH[28], and FDH[70]) render similar results. In the previous in vacuo studies, we predicted that the computed KIE were in good agreement with experimental data when the reactants were moulded into the quadratic zone of the saddle point structure. In this QM/MM study we have already pointed out how a more realistic reactants-like structure is located, where pteridine and dihydronicotinamide rings are compressed. The relative orientation imposed by the active site constrains the reactants close to the quadratic region of the TS.

The analysis of the normal modes frequencies of the TS yields a relatively high imaginary frequency (see Table 1), mainly associated with forming/breaking bonds. The dominant amplitudes of this vector are related to the interatomic distances of donor and acceptor carbons, the Ht, advance and the angle controlling the position of the secondary hydrogen (H4 of didydronicotinamide ring). The visualization of the imaginary normal mode provided by GRACE and interfaces such as RASMOL[71] or XMOL[72] allows one to check how this frequency is also associated to planar-boat movement of the dihydronicotinamide moiety, as the rehybridization of the ring is changing from reactants to TS. These results reveal that the primary and secondary KIE are strongly coupled, in agreement with experimental data. This result justifies the use of a minimal set of coordinates capable of producing most of the TS features. Other normal modes, corresponding to the second, third, etc. eigenvalues, are significantly smaller (ca. 100 and 60 cm^{-1} for the in vacuo and the QM/MM calculations, respectively) revealing quite soft movements. This result shows that the force constants are getting smaller if we move from the simple models used in vacuo to the model where the complete protein surroundings is modeled. We can consider that the active site helps the system in softening the vibrational degrees of freedom, while it keeps invariant the geometry and transition vector amplitudes. This trend was also observed in a very recent work[31] where a comparative in vacuo versus QM/MM study was carried out for the oxygenation step of the rubisco enzyme mechanism.

Conclusions

In this paper we present a theoretical study of the hydride transfer step in dihydrofolate reductase. The hybrid quantum-mechanical/molecular-mechanical (AM1/CHARMM24/TIP3P) technique used has allowed to include the protein environment to be included and the structural features of significance on hypersurfaces spanning several thousand degrees of freedom to be explored. We focus our interest on the transition structure, which has been located and characterized involving a fully flexible active-site region by means of GRACE software. The results have been compared with semiempirical (AM1) and ab initio (HF/4-31G) in vacuo calculations to stressed the importance of including the environment effect. Theoretical predictions, including KIE, have been compared with previous published experimental data. The analysis of the results can be summarized as follows.

While the gas-phase calculations render an endo and an exo transition structure, this degeneracy is not obtained when the protein environment is included: the enzyme selectively moulds the substrate in a conformation close to the exo transition structure.

From the comparison between the reactant-like structures obtained in vacuo and by means of the hybrid technique it can be concluded that the enzyme compresses the substrate and the cofactor into a conformation close to the transition structure, thus facilitating the hydride transfer.

The population analysis obtained by means of the in vacuo and the hybrid QM/MM methods renders similar net atomic charges for the donor and acceptor fragments, suggesting that a hydrogen more than a hydride ion is transferred.

The QM/MM calculations allow the role of the Asp27 in stabilizing the cationic pteridine ring to be demonstrated, while the ordered structure of the X-ray crystallographic water molecules supports the hypothesis of an indirect transfer of a proton from the Asp27 residue to the N5 atom of the substrate.

Good agreement between experimental and semiclassical QM/MM primary kinetic isotope effects is found. Nevertheless, this conclusion must be considered with caution as the hydride transfer step in DHFR is not the rate-limiting step at the pH at which modeling has been carried out.

Finally, the comparison of the results obtained with the different methods and models shows that while some common features are observed, for reactions involving a large number of degrees of freedom it is not correct to refer to one unique transition structure. The transition state should be considered as an average of nearly degenerated transition structures.

(67) Williams, I. H. *Chem. Phys. Lett.* **1982**, 88, 462.
(68) Williams, I. H. *J. Mol. Struct. THEOCHEM* **1983**, 11, 275.
(69) Tapia, O.; Cardenas, R.; Andrés, J.; Colonna-Cesari, F. *J. Am. Chem. Soc.* **1988**, *110*, 4046.
(70) Tapia, O.; Andrés, J.; Cardenas, R. *Chem. Phys. Lett.* **1992**, *189*, 395.
(71) Sayle, R. Rasmol v2.5: A molecular visualisation Program, Biomolecular Structure, Glaxo Research and Development: Greenford, Middlexsex, UK.
(72) Xmol version 1.3.1, Minnesota Supercomputer Center Inc.

Acknowledgment. We are indebted to DGICYT for project PB96-0795-C02-02 which supported this research, and the Servei d'Informatica of the Universitat Jaume I for providing us with computer capabilities. The authors warmly thank Professors Ian H. Williams and O. Tapia for helpful discussion.

JA9843019